Analyzing spatial and temporal evolution of groundwater salinization through multivariate statistical analysis and hydrogeochemical facies evolution-diagram

Analyzing spatial and temporal evolution of groundwater salinization through Multivariate Statistical Analysis and Hydrogeochemical Facies Evolution-Diagram

Alessandro Parisi[1,2*], Maria Rosaria Alfio[1], Gabriella Balacco[1], Cüneyt Güler[3], Maria Dolores Fidelibus[1]

[1] Dipartimento di Ingegneria Civile, Ambientale, del Territorio, Edile e di Chimica (DICATECh), Politecnico di Bari, Bari, 70125, Italy

[2] Dipartimento di Ingegneria Elettrica e dell'Informazione (DEI), Politecnico di Bari, Bari, 70125, Italy

[3] Mersin Üniversitesi, Çiftlikköy Kampüsü, Jeoloji Mühendisliği Bölümü, Mersin, 33343, Turkey

[*] Corresponding Author: alessandro.parisi@poliba.it

ABSTRACT

The growing groundwater withdrawal rates in coastal aquifers in arid/semi-arid regions exacerbate seawater intrusion and saltwater upconing by causing groundwater salinization and potential adverse and cascading effects to related groundwater-depending systems. This study aims to highlight the dynamics of groundwater salinization in time and space by comparing the efficacy of statistical (hierarchical cluster and factor analyses) and hydrogeochemical (hydrogeochemical facies evolution) methods. Multi-temporal groundwater samples collected from the monitoring well network in the study area (Salento Aquifer, Puglia region, Southern Italy) have been considered to recognize such dynamics. By comparing the spatial and temporal evolution of water clusters, factor scores, and hydrogeochemical facies, the proposed methodological approach enables the identification of zones characterized by the low dynamics of freshening and intrusion processes (with invariant features during the investigated period), which correspond to groundwater recharge areas and zones subject to groundwater salinization respectively. On the contrary, a high spatial and temporal variability of salinization dynamics typifies the zones subject to alternation of groundwater characteristics. These results allow outlining of a preliminary hazard

map related to groundwater salinization processes, which might be a useful tool for policymakers and stakeholders involved in groundwater management of coastal aquifers. Results suggest that generally, a thoughtful understanding of limitations concerning the aquifer heterogeneity and anisotropy, distribution and density of control points, and depth of sampling is crucial for handling the study outcomes, especially for the aims of management.

Keywords: Hierarchical Cluster Analysis, Factor Analysis, HFE-Diagram, Groundwater salinization, Freshening/Intrusion substages

1. Introduction

Groundwater from coastal aquifers along the Mediterranean coast represents the most important resource for the water supply. In such aquifers, groundwater abstraction often exceeds the natural recharge rate causing a hydrodynamic and hydrochemical imbalance, which, in turn, triggers lateral seawater intrusion in the coastal zone and saltwater upconing inland (Tulipano et al., 2005; Custodio, 2010; Werner et al., 2013; Gleick et al., 2014; Leduc et al., 2016; Mastrocicco and Colombani, 2021).

Because of common climatic and social conditions, groundwater salinization in arid/semi-arid regions is the major concern for many coastal aquifers (Custodio and Bruggeman, 1987; Pulido-Bosch et al., 1991; Domínguez and Custodio, 1992; Flores-Marquez et al., 1998; Bear et al., 1999; Petalas and Lambrakis, 2006; Giménez-Forcada, 2010; Bouderbala, 2015; Tamez-Meléndez et al., 2016; Telahigue et al., 2018; Mastrocicco and Colombani, 2021; Muzzillo et al., 2021). In addition, because of the complex interdependence between groundwater and related ecosystems, the deterioration in quality and quantity of the former may lead to cascading consequences and crises for the latter (Pescaroli and Alexander, 2015; Parisi et al., 2018). In the context of water resources management, such complex interconnections raise serious concerns about the potential cascading vulnerabilities of groundwater-dependent systems in coastal areas (Pescaroli et al., 2018).

Since groundwater salinization changes over time and space due to fluctuations in natural and human pressures, it is essential to evaluate the variability of physical and chemical parameters in groundwater by frequent monitoring. Graphical methods, such as Stiff (1951), Piper (1944), and Schoeller

53 (1955) diagrams, may allow evidence for dynamic conditions, recognition of mixing processes, and
54 linked water-rock interactions by grouping water samples of different monitoring periods according to
55 similar chemical features. However, when dealing with large datasets and long monitoring records, these
56 graphical methods have some inherent limitations (see Güler et al., 2002).
57 A few methodological approaches can handle multi-temporal monitoring data to highlight the
58 dynamics of concerned processes. A suitable method is the Hydrochemical Facies Evolution-Diagram
59 (HFE-D) conceptualized by Giménez-Forcada (2010), where each hydrochemical facies is typical of a
60 phase of salinization or freshening (see Bahir et al., 2018; Sappa et al., 2019; Sae-Ju et al., 2020; Hajji et
61 al., 2021; Roy and Zahid, 2021). The HF distribution over time provides information on the temporal
62 variation of the groundwater salinization phenomenon (Giménez-Forcada 2014; 2019). Multivariate
63 statistical analysis (MVSA) is another valuable method that might be useful for this purpose. MVSA
64 allows the handling of many geochemical and physical parameters (variables) for grouping water samples
65 showing similarities into homogeneous clusters (Güler et al., 2002; Ghesquière et al., 2015; Machiwal et
66 al., 2018). MVSA may also help in disclosing spatial and temporal variability of groundwater quality,
67 identifying the major hydrochemical processes, and assessing their temporal evolution (see Güler et al.,
68 2002; Papatheodorou et al., 2007; Pacheco Castro et al., 2018; Bahrami et al., 2020; Prusty and Farooq,
69 2020).
70 Given the above, this study aims at highlighting the dynamics of groundwater salinization in time
71 and space by comparing the efficacy and results of HFE-D and MVSA (i.e., Hierarchical Cluster Analysis
72 (HCA) and Factor Analysis (FA)) in recognizing such dynamics. In this work, a karstic coastal aquifer
73 (Salento aquifer (SAL)) located in the Mediterranean basin (Puglia region, Southern Italy) has been
74 selected as a case study, due to its well-known and worrying salinization phenomenon (Tadolini et al.,
75 1982; Tulipano and Fidelibus, 2002; Cotecchia, 2014; Polemio, 2016). This study proceeded according to
76 the following steps: (i) selection of chemical analyses (sampling survey periods and validation of related
77 groundwater analyses) and compilation of the dataset; (ii) application of HFE-D method to the dataset;
78 (iii) clustering of water samples that show similarities based on their parameters (Q-mode HCA), (iv)
79 grouping of parameters showing similarities based on chemical analyses of water samples (R-mode FA);
80 (v) mapping the results of geochemical and of statistical approaches for each monitoring period; (vi)

comparison of results from HFE-D and MVSA methods and assessment of the potential of both methods in outlining temporal and spatial dynamics of groundwater salinization.

2. Study area: Salento aquifer (Puglia region, Southern Italy)

The dataset composed of physical and chemical parameters involved in this study concerns groundwater samples collected from the karstic coastal aquifer of the Salento Peninsula (Puglia region, Southern Italy). The SAL aquifer extends from the Ionian to the Adriatic Sea (Fig. 1a). Its limit coincides with those of the Lecce Province, which is a highly urbanized area where the agricultural land occupies about 80% of the total area. Mild, relatively rainy winters and hot and dry summers characterize the climate in this region. Most of the Salento Peninsula suffers from frequent drought periods, which affect groundwater resources (Balacco et al., 2022). As shown by Alfio et al. (2020), the percentage of the territory affected by drought periods increased between 1980 and 2011 compared to the previous 30 years. Due to a lack of surface water resources, groundwater from the SAL aquifer is almost the only resource for domestic, agricultural, and industrial water supply in the region (Regione Puglia, 2005; 2015). Thus, preserving the groundwater quality of the coastal aquifer of the Salento Peninsula plays a crucial role in the water management in this area. Due to its coastal setting, the SAL aquifer has a long-standing issue of groundwater salinization, whose dynamics is the key knowledge to prevent potential negative and cascading effects on groundwater-dependent environmental, economic, social, and ecological systems (Parisi et al., 2018).

2.1 Geological and hydro-lithological settings

The carbonate formation (layers and banks of fractured and karstified limestone) of the Upper Cretaceous–Paleocene belonging to the Mesozoic carbonate platform called the “Apulian platform” constitutes the geological basement of the SAL aquifer. Tectonics caused a combination of gentle folds, as well as strike-slip and normal faults, leading to the break-up and dislocation of the carbonate basement and spatial variability of the transgressive processes. The complex fault system determines Horst and NW-SE oriented Graben structures: the Horsts of the Mesozoic basement emerge in the SW portion of the so-called “Serre Salentine” (Ionian side) showing elevations around 200 m AMSL, while Neogene and

Quaternary sediments in the eastern portion (Adriatic side) fill the Grabens (Fig. 2). According to the classification of Struckmeier and Margat (1995), the carbonate formation hosting the SAL aquifer corresponds to an “extensive but only moderately productive aquifer”, whereas the covering strata range from “minor aquifers with local and limited groundwater resources” to “strata with essentially no groundwater resources” (Fig. 1b).

A wide endorheic area, which corresponds to the main recharge area of the SAL aquifer, marks the territory with hundreds of dolines, with or without clear swallow holes at their bottoms (Fig. 1a). The recharge mechanisms are complex, being conditioned by the multifaceted permeability structures formed by epikarst, low permeability unsaturated zone, karst surface and subsurface features, fracture zones, and major faults.

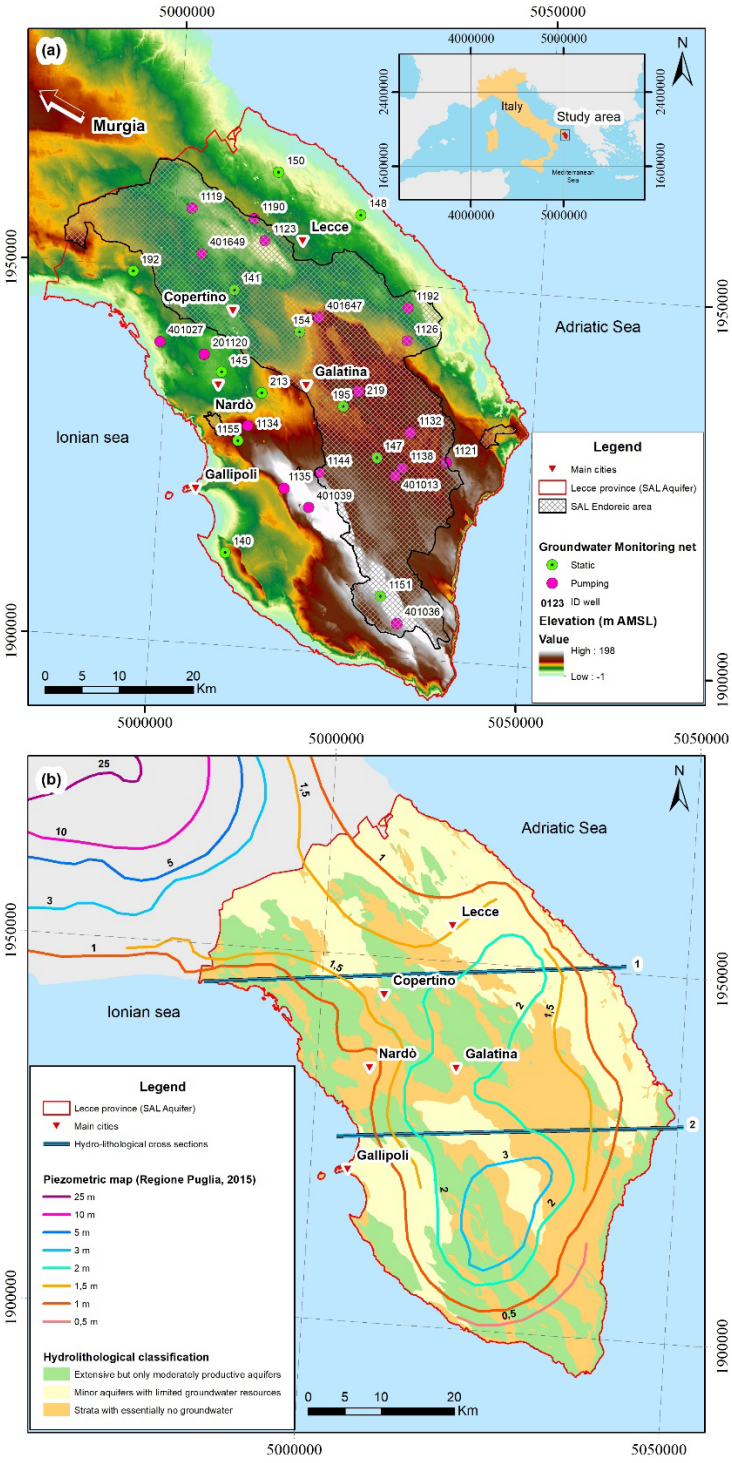

Figure 1. (a) Study area and groundwater monitoring network with wells in static and pumping conditions; (b) Hydro-lithological map of SAL aquifer according to the classification of Struckmeier and Margat (1995), piezometric map (from Regione Puglia, 2015) and traces of the hydro-lithological cross sections (see Fig. 2). Coordinates are in ETRS89-LAEA reference system.

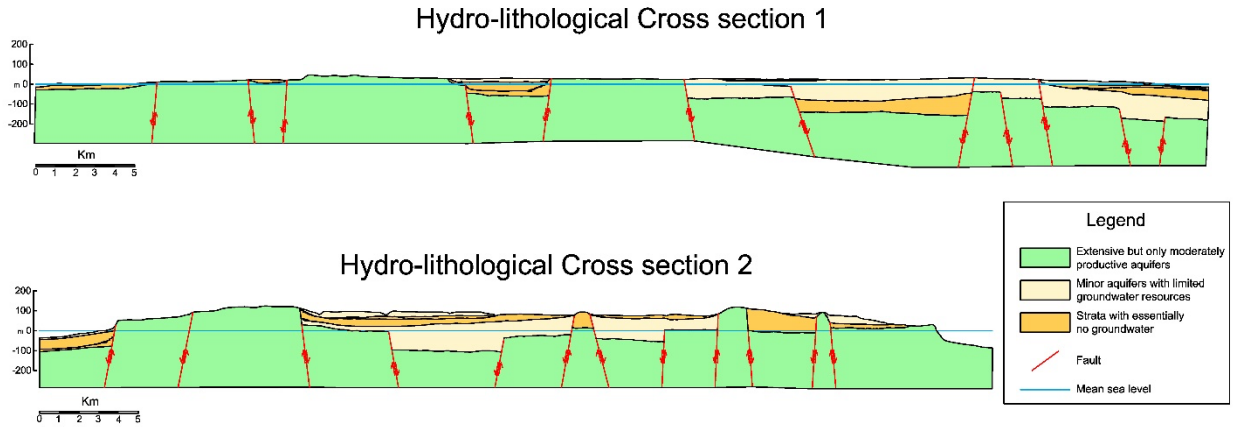

Figure 2. Hydro-lithological cross sections 1 and 2 (location in Fig. 1b) of SAL aquifer according to the classification of Struckmeier and Margat (1995) and major faults.

2.2 Groundwater salinization and the regional monitoring well network

Groundwater salinization is one of the major issues related to the SAL aquifer and it is mostly due to saltwater upconing caused by intense groundwater exploitation (Tadolini et al., 1982; Tulipano and Fidelibus, 2002). Because of the estimated high number of unlicensed wells (Regione Puglia, 2005), the actual amount of groundwater abstraction from the SAL aquifer is unknown. Saline groundwaters, which are present all over the Salento Peninsula, show chemical and isotopic features deeply different from those of present seawater. Their apparent ages are as high as 15,000 years (Fidelibus et al., 2011), and likely date back to the last Flandrian regression. Lateral seawater intrusion only occurs around a few stretches of the coastline, while most groundwaters subject to salinization show the fingerprint of old saltwater (Fidelibus and Tulipano, 1986).

The highest hydraulic heads (from 2 to 3 m AMSL) occupy the central part of the aquifer, suggesting the existence of a regional flow system (Fig. 1b). To the NW, groundwater flows towards an intermediate zone, which works as a buffer zone, where the flows from the contiguous Murgia aquifer and the SAL aquifer mix. Although hydraulic heads appear to be interconnected at the regional scale, the likely barrier role exerted by the major faults suggests compartmentalization of the aquifer (Fidelibus and Pulido-Bosch, 2019). Discharge into the sea occurs through diffuse fronts or brackish coastal springs depending on the type of permeability of the carbonate rocks along the coast (owing to fracturing, fissuring, and/or karstification) and any confining layers that might prevent direct contact with seawater.

A comprehensive groundwater monitoring program in the SAL aquifer started only in 1994 based on the Regional Monitoring Network (RMN) set by the Puglia Regional Government. In the last 30 years, according to variable protocols and involved wells, the monitoring efforts included sampling with bailers at different depths in static wells, direct sampling in pumping wells, multi-parameter logs, water level measurements, and continuous registration with sensors in some wells under static (non-pumping) conditions. The most recent monitoring program that concerns the SAL aquifer (Maggiore Project) started at the end of 2015. It includes up to present groundwater sampling campaigns carried out with a semi-annual frequency from 2016 to 2018. The RMN of the SAL aquifer includes 57 wells, of which 22 are public wells in static condition and 35 are private wells equipped with pumps, normally used for domestic or irrigation purposes. Well depths vary from 40 m to 290 m according to the geological and hydrogeological setting of each well location. Sampling always occurs at a fixed depth for each well during each monitoring survey; the fixed depth for pumping wells coincides with the depth of the pumps. The consistency of sampling depths makes feasible the comparison between water samples over time. Since sampling depths refer to the most productive levels of the aquifer (Regione Puglia, 2005; 2015), groundwater samples collected from the RMN of the SAL aquifer may be considered representative of the overall qualitative and quantitative status of the groundwater body.

3. Materials and methods

3.1 Sampling and analysis

The chemical analyses of groundwater considered for this study were sourced from six monitoring surveys carried out from 2016 to 2018 within the Puglia water monitoring program named “Maggiore Project”. The monitoring program had a semi-annual frequency, with sampling at the end of each wet season (from April to June), as well as at the end of each dry season (from September to early December). The six monitoring surveys concerning the SAL aquifer comprise 290 groundwater samples (collected from 22 static and 35 pumping wells) analyzed for various physical and chemical parameters.

The water chemistry dataset was subjected to data screening based on pre-selected criteria. For instance, water samples that did not satisfy a specified Charge Balance Error (CBE) were excluded from further evaluation. Since the dataset included many water samples with high salinity, a CBE within ±10%

was deemed acceptable (see Güler et al., 2002). Then, to allow a comparison of water quality over time, groundwater samples collected from those wells that were not sampled in all six surveys were excluded. The final dataset obtained after data screening comprises water samples collected from 31 monitoring wells (12 static and 19 pumping wells) with repeated sampling in the six sampling periods (three wet and three dry seasons) (Fig. 1a).

Laboratory analyses were carried out by ARPA Puglia (Regional Agency for Environmental Prevention and Protection, https://www.arpa.puglia.it/) according to the analytical methods available at https://www.arpa.puglia.it/pagina3128_qualit.html. The chemical analyses concerned major cations (Ca^{2+}, Mg^{2+}, Na^{+} and K^{+}) and anions (Cl^{-}, SO_4^{2-}, NO_3^{-} and HCO_3^{-}), as well as some minor ions (NH_4^{+}, NO_2^{-}, PO_4^{3-}, Br^{-} and F^{-}). The physical parameters, including temperature, pH, electrical conductivity (EC) and dissolved oxygen (DO) were measured in situ by technicians of the ARIF Puglia (Regional Authority of Puglia involved in groundwater sampling and monitoring, https://www.arifpuglia.it/) utilizing daily calibrated portable multi-parameter probes.

3.2 Application of MVSA techniques and data processing

In this study, MVSA techniques such as Q-mode HCA and R-mode FA were respectively used to classify groundwater samples based on their similarities in physicochemical characteristics (see Güler et al., 2002) and to decipher associations among selected water chemistry variables (see Machiwal et al., 2018). The selection of these MVSA techniques is based on their ability to provide new insights into multivariate datasets, such as the one compiled within the framework of the current study. As a preliminary step, the water chemistry dataset was examined regarding censored and missing data values, since such datasets are not suitable for MVSA applications (Farnham et al., 2002). For the replacement of censored concentration values recorded as "less-than", the technique suggested by Sanford et al. (1993) was used, where the lower detection limit of the instrument is multiplied by 0.55. In this study, the parameters with censored or missing values exceeding 15% were excluded from further statistical analyses. In the second step, the statistical distribution of parameters was checked using the Kolmogorov-Smirnov test (Kolmogorov, 1933; Smirnov, 1948), since both MVSA techniques require normalization and standardization of parameters involved in the analysis (Alther, 1979; Romesburg, 1984; Reimann and

Filzmoser, 2000). Parameters with non-normal distribution were subjected to Box-Cox transformation (Box and Cox, 1964; 1982). If a parameter showed a non-normal distribution even after the Box-Cox transformation, it was not used in the subsequent statistical analyses. Finally, all parameters displaying a normal distribution were standardized by calculating their standard scores (*z*-scores), which ensures an equal weight of each parameter in the statistical analysis (Johnson and Wichern, 1992; Güler et al., 2002).

In Q-mode HCA, Ward's method (Ward, 1963) was used as the linkage method to assess the similarities among members of water groups (i.e., clusters). The resulting hierarchical dendrogram (Davis, 1986) was used to visualize Q-mode HCA results, where the horizontal line (a.k.a. phenon line) drawn across the dendrogram branches identifies the number of clusters. Box plots of the clusters, as well as maps related to each monitoring survey, were used to represent distinctive features of the statistically defined water groups (i.e., clusters).

In this study, R-mode FA was used to establish the correlation structure among the observed (original) variables and to extract unobserved (latent) variables named factors (Dalton and Upchurch, 1978; Basilevsky, 1994). The sampling adequacy test of Kaiser-Meyer-Olkin (KMO) was applied to determine the suitability of the compiled database for FA application (Kaiser, 1974; 1981). KMO values are considered acceptable, if greater than 0.5, whereas the KMO values close to unity define the best FA application related to the dataset. The number of factors summarizing the key processes related to the database was selected according to the "Explained variance criterion". In this study, an orthogonal varimax rotation was applied for maximizing the loading related to one factor and minimising the loading related to the others (Davis, 1986). Then, the factor loading matrix was examined to define variable-factor associations, as well as to describe the hydrogeochemical process associated with each latent factor, where the higher the factor loading (close to ± 1), the higher the influence of variables on the respective factor. Conversely, factor loadings close to zero identify a weak correlation between the variables and factors. The maps displaying the spatial distribution of the factor scores (FSs), which are related to the intensity of the process underlying each factor (Dalton and Upchurch, 1978), were prepared for each groundwater survey to show their variation over time.

3.3 Hydrogeochemical Facies Evolution-Diagram (HFE-D)

The Hydrogeochemical Facies Evolution-Diagram (HFE-D) proposed by Giménez-Forcada (2010; 2014) allows for exploring the hydrogeochemical variations that occur over time by groundwater freshening and salinization processes (available at https://hidrologia.usal.es/HFE-D.htm). The diagram includes four main "heteropic" facies ($NaHCO_3$, NaCl, $CaHCO_3$, and CaCl), which are defined by coupling sodium or calcium, and chloride or bicarbonate percentages when higher than 50%. Moreover, it includes mix facies, which represent facies where the named ion is higher than any other ion but it is less than 50% (Giménez-Forcada, 2010; 2014; Giménez-Forcada and Sánchez-San Román, 2015). The abscissae of the HFE-D separately mark the percentages of Na^+ and Ca^{2+}, aiming to recognize heteropic hydrochemical facies (HFs - as $NaHCO_3$ and CaCl) and mix facies that occur in coastal aquifers under the effects of base-exchange reactions triggered by mixing of fresh- and salt-waters. The percentage of chloride in the ordinate traces groundwater salinization, while the percentage of bicarbonate or sulfate (depending on the dominant anion in freshwater) typifies the HFs typical of groundwater recharge. The Conservative (or non-reactive) Mixing Line (CML), built with a freshwater end-member and a saline water end-member (usually seawater), separates the freshening phases and facies, which are located to the left above the CML, and the intrusion phases and facies, which are to the right under the CML. Different sub-stages related to freshwater and intrusion phases can be identified in accordance with the chemical composition of sampled waters. Both freshening sub-stages (from the beginning to the end of the freshening process are f1, f2, f3, f4 and FW) and the intrusion sub-stages (from the beginning to the end of the intrusion process are i1, i2, i3, i4 and SW) help to identify the salinization dynamics of groundwater samples (Giménez-Forcada, 2014; 2019).

The position of the CML in the HFE-D is crucial for the water sample classification. In this work, since the groundwater salinization is mostly due to saltwater upconing caused by intense groundwater exploitation (Tadolini et al., 1982; Tulipano and Fidelibus, 2002), we defined the concentrations of the major ions of the saline end-member as the average of chemical analyses associated with saline water samples collected in past monitoring programs (1986) in deep wells reaching saltwater beneath freshwater in the study area (Fidelibus et al., 2011 – data is available from the MEDSAL Observatory at

https://medsal.eu/observatory/). Regarding the freshwater endmember, the HFE-D model automatically selects the chemical composition of the freshest groundwater collected during the six sampling surveys.

By the HFE-D, each water sample collected from the 31 monitoring wells of Lecce province from 2016 to 2018 was classified according to a freshening or intrusion HF. Finally, the HFs distribution was plotted for each survey on maps following the methodological approach proposed by Giménez-Forcada (2010; 2014; 2019).

4. Results

Concerning MVSA methods (Q-mode HCA and R-mode FA), some variables were excluded after checking missing/censored values and the natural range of measured values. Groundwater temperature was not considered because measured values were out of the natural range. The variables NH_4^+, NO_2^-, PO_4^{3-}, Br^- and F^- were also excluded due to a high percentage (>15%) of censored values (concentrations below the detection limit). Since the aim of the present work is related to the dynamics of groundwater salinization, nitrate (NO_3^-) was not considered in the multivariate statistical analyses, because it does not represent a natural process, but rather a parameter linked to anthropogenic activities (Rahman et al., 2021). No missing values were present in the dataset. MVSA applications for the SAL aquifer were conducted considering the physical and chemical variables that include EC, DO, pH, Ca^{2+}, Mg^{2+}, Na^+, K^+, Cl^-, SO_4^{2-}, and HCO_3^-. Table 1 summarizes the statistical results obtained from R-Studio Software (R Core Team, 2019) on the considered parameters. Some parameters (EC, Mg^{2+}, Na^+, K^+, Cl^- and SO_4^{2-}) showed a non-normal distribution according to the Kolmogorov-Smirnov test. Therefore, these parameters were subjected to a data normalization step using the Box-Cox transformation, followed by the Kolmogorov-Smirnov test. Since SO_4^{2-} and K^+ are not normally distributed, even after Box-Cox transformation, they were not considered in statistical analyses.

Fig. 3 shows the dendrogram resulting from Q-mode HCA applied to all sampling periods and the selected variables. Since the chosen dissimilarity value was about 17, three clusters of groundwater samples were obtained. To illustrate the differences between the clusters resulting from HCA, Box plots concerning all major ions and total dissolved solids (TDS) were plotted for each group derived by Q-mode HCA (Fig. 4). It is worth mentioning that ions excluded from the statistical analysis (NO_3^-, SO_4^{2-}

278 and K^+) were also represented in Fig. 4 only for comparison purposes. Table 2 reports the median values
279 of major ions for each cluster obtained by Q-mode HCA.
280
281 Table 1. Statistical summary of parameters considered in MVSA applications. Variables *in italics* and
282 underlined were not included in the following steps because of their non-normal distribution even after
283 the data normalization step.

Parameter	Unit	Min.	Max.	Mean	Median	Standard deviation	*p*-value	Box-Cox λ	Box-Cox *p*-value
EC	µS/cm	389	13,920	1,484.4	1,092.5	1,451	<0.05	-0.495	0.28
DO	mg/L	2.82	10.57	8.31	8.52	1.14	0.164	NA	NA
pH	Standard	6.91	9.36	7.47	7.40	0.34	0.885	NA	NA
Ca^{2+}	mg/L	3.70	274.00	86.31	80.40	36.49	0.446	NA	NA
Cl^-	mg/L	16.00	5,026	321.25	176.50	552.37	<0.005	-0.147	0.277
HCO_3^-	mg/L	132.00	488.00	309.77	311.00	69.77	0.665	NA	NA
K^+	*mg/L*	*0.55*	*92.00*	*9.41*	*5.85*	*12.52*	*<0.05*	*-0.049*	*<0.05*
Mg^{2+}	mg/L	3.80	319.00	42.69	35.00	38.04	<0.05	0.08	0.194
Na^+	mg/L	10.00	2,703.00	176.51	108.00	296.60	<0.05	-0.112	0.137
SO_4^{2-}	*mg/L*	*5.00*	*609.00*	*58.11*	*38.00*	*79.12*	*<0.05*	*-0.047*	*<0.05*

284
285 The R-mode FA extracted three significant factors, which explained 79.2% of the total variance in
286 the dataset. As shown in Table 3 concerning the varimax rotated factor loadings, the salinization process
287 (related to EC, Na^+, Mg^{2+} and Cl^-) is the most significant factor (F1). As our focus is on the salinization
288 processes, only FSs related to F1 have been further investigated and compared with other findings.
289 Fig. 5 shows the HFE-Diagram with substages of freshening/intrusion processes for all water
290 samples. Figs. 6 and 7 show the thematic maps of the F1 scores (for each monitoring survey) associated
291 with groundwater salinization (left-hand side), as well as the interpolation of the hydrogeochemical facies
292 related to the different substages of freshening/intrusion processes (right-hand side) carried out following
293 the methodological approach proposed by Giménez-Forcada (2014). Both results are compared with those
294 from the cluster analysis derived by Q-mode HCA (Fig. 3).
295

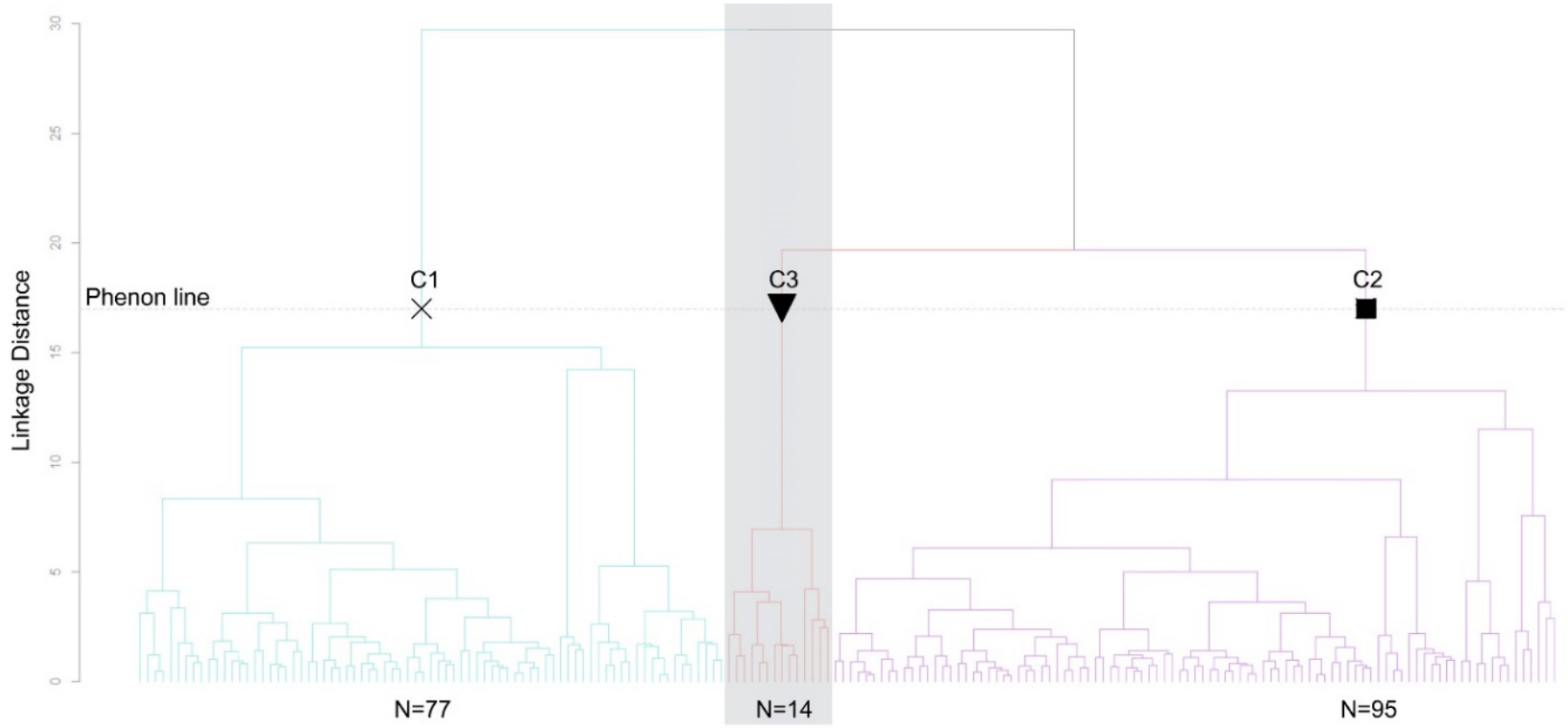

296

297 Figure 3. Dendrogram of Q-mode HCA. The dashed line represents the selected level of dissimilarity (17), which identifies three clusters: C1, C2 and C3.

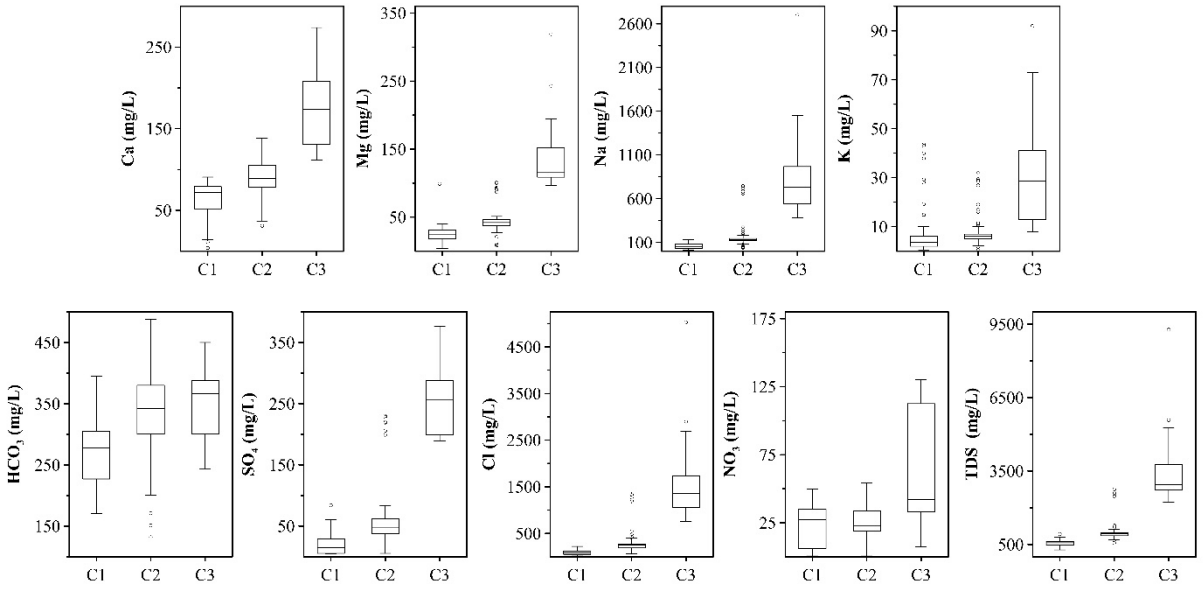

Figure 4. Box plots for major ions and TDS for each cluster (C1, C2 and C3) derived by Q-mode HCA.

Table 2. Median values of physical and chemical parameters for each cluster derived by Q-mode HCA (The parameters that were not included in MVSA methods are presented only for comparison purposes).

HCA Group	Unit	C1	C2	C3
EC	µS/cm	792.00	1,347.00	4,145.00
DO	mg/L	8.65	8.41	7.86
pH	Standard	7.55	7.36	7.28
TDS	mg/L	567.20	933.40	2,938.00
Br^-	mg/L	0.40	0.60	4.70
Ca^{2+}	mg/L	72.00	89.00	173.50
Cl^-	mg/L	75.00	246.00	1,365.00
F^-	mg/L	0.19	0.20	0.21
HCO_3^-	mg/L	278.00	342.00	366.00
K^+	mg/L	3.60	6.00	28.75
Mg^{2+}	mg/L	24.00	42.60	115.35
Na^+	mg/L	47.00	134.00	730.00
NH_4^+	µg/L	27.50	27.50	98.75
NO_2^-	µg/L	27.50	27.50	27.50
NO_3^-	mg/L	27.00	24.00	42.00
PO_4^{3-}	mg/L	0.55	0.55	0.55
SO_4^{2-}	mg/L	15.00	47.00	257.00

Table 3. Varimax rotated factor loadings, eigenvalues, and total and cumulative variance related to the dataset.

Parameters	Factor 1	Factor 2	Factor 3
EC	**0.930**	0.213	0.105
DO	-0.148	-0.014	0.024
pH	-0.036	**-0.934**	-0.141
Cl^-	**0.968**	0.136	0.029
Ca^{2+}	0.513	**0.665**	0.178
Mg^{2+}	**0.896**	0.116	0.190
Na^+	**0.973**	0.053	0.046
HCO_3^-	0.147	0.214	**0.963**
Eigenvalue	4.37	1.38	0.91
% Total variance	48.26	18.02	12.89
% Cumulative variance	48.26	66.28	79.17

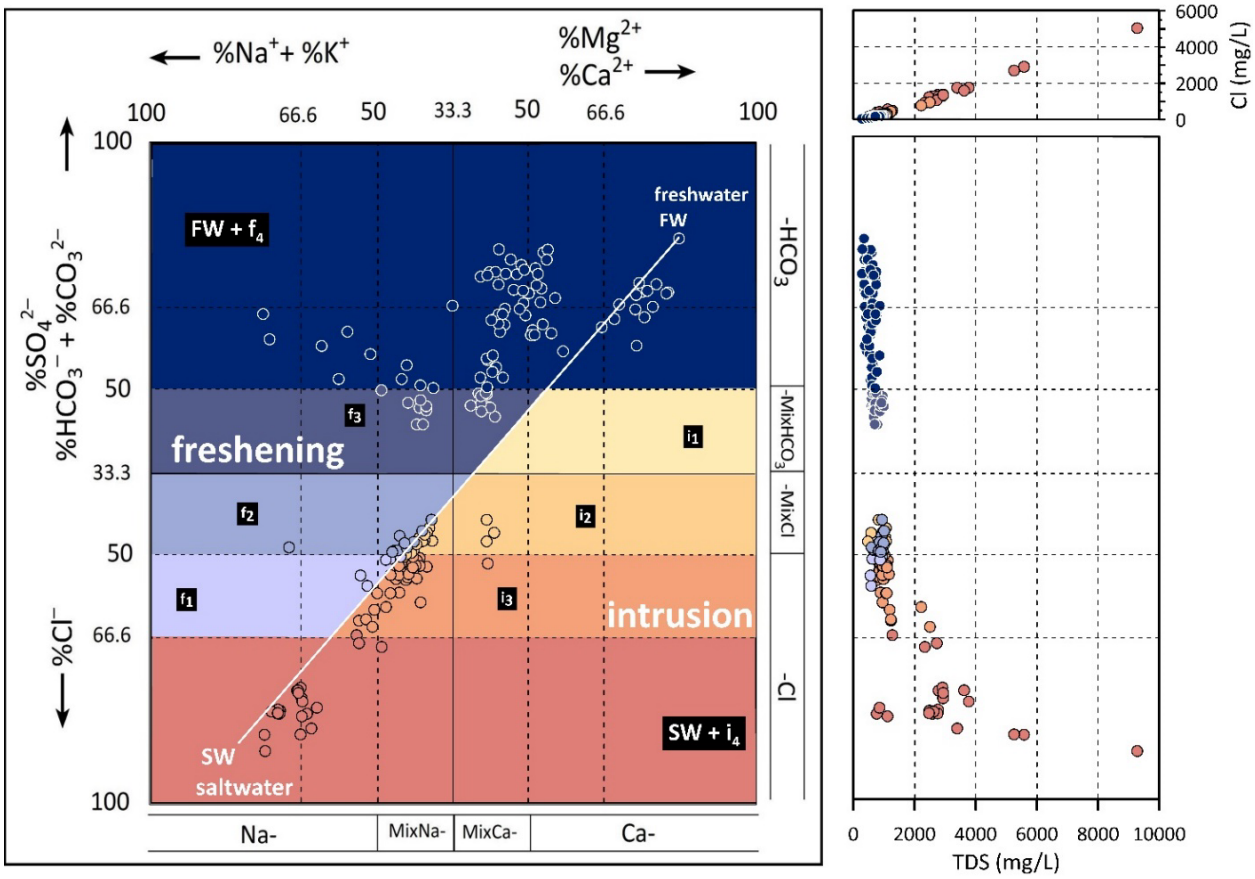

Figure 5. HFE-Diagram of the chemical analyses for the six sampling surveys. The diagrams on the right-side add information about the TDS and chloride concentration related to the freshening and intrusion HFs (Giménez-Forcada, 2014; 2019)

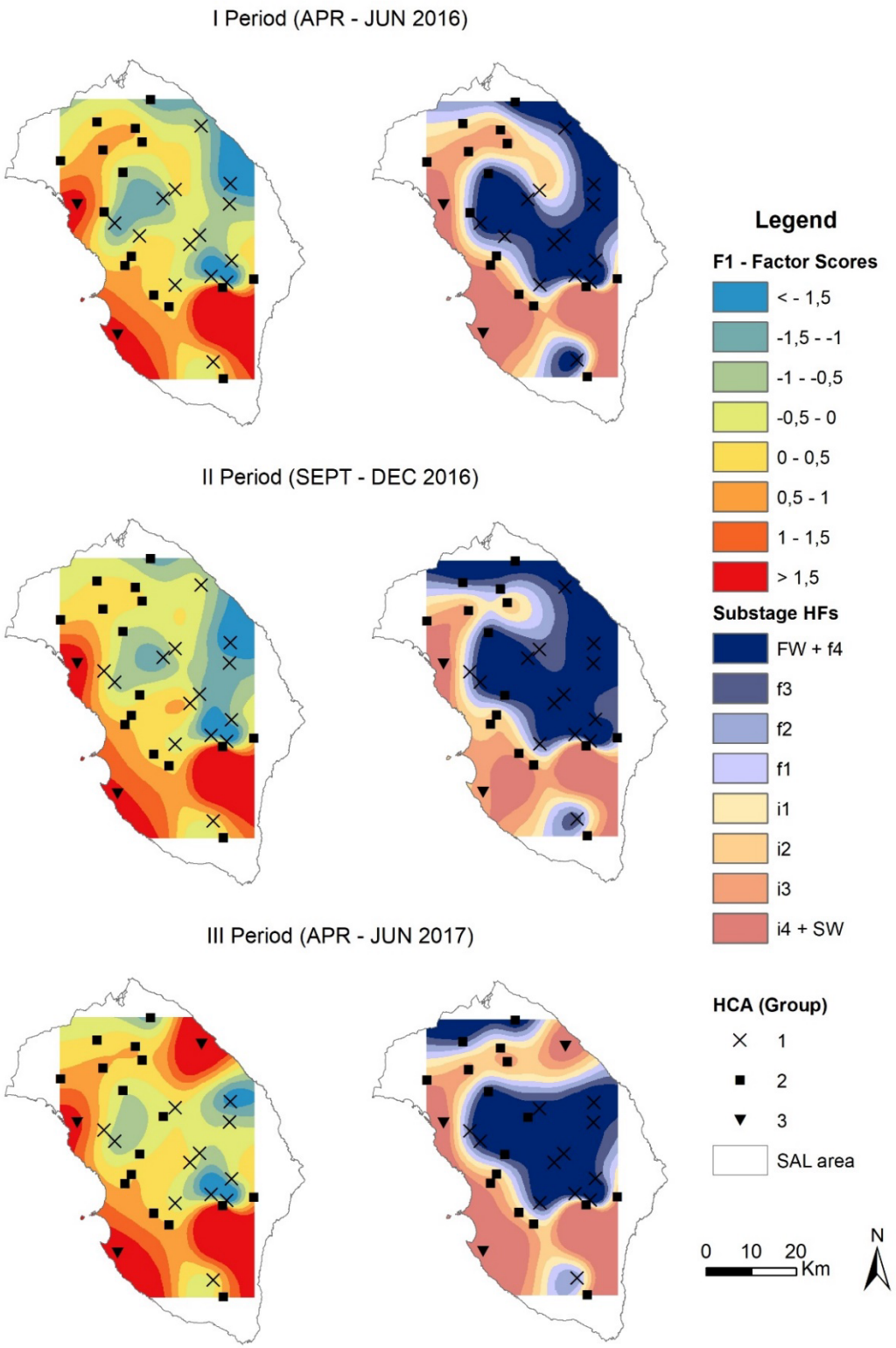

311

312 Figure 6. Results of R-mode FA, HFE-D and Q-mode HCA are shown for the sampling periods I, II and III.

313 On the left-hand side, the thematic maps are associated with FSs of F1 (groundwater salinization) derived by

314 R-mode FA; on the right-hand side, the thematic maps are associated with HFs derived by the HFE-D. On

315 both sides, results derived by Q-mode HCA.

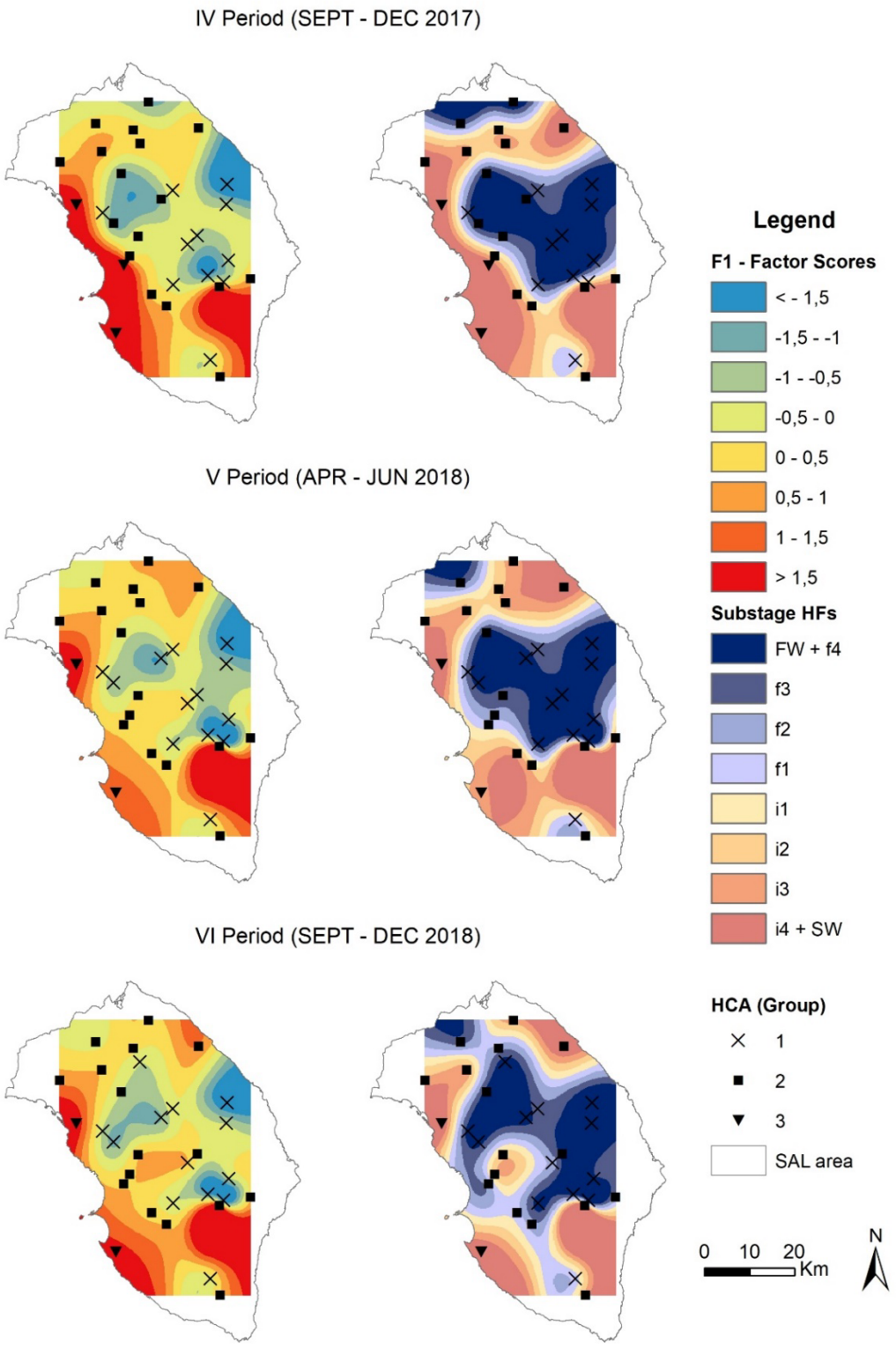

316

317 Figure 7. Results of R-mode FA, HFE-D and Q-mode HCA are shown for the sampling periods IV, V and
318 VI. On the left-hand side, the thematic maps are associated with FSs of F1 (groundwater salinization)
319 derived by R-mode FA; on the right-hand side, the thematic maps are associated with HFs derived by the
320 HFE-D. On both sides, results derived by Q-mode HCA are shown.

5. Discussion

Q-mode HCA enabled the grouping of 186 groundwater samples (see Fig. 3) collected from 2016 to 2018 during six sample surveys concerning 31 monitoring wells of the SAL aquifer. As a result, three clusters (C1, C2 and C3) were identified by the selected level of dissimilarity (17), which is based on a graphical examination of the dendrogram. Fig. 4 and Table 2 display (for each cluster) the variation of parameters considered for clustering and those excluded from the statistical analysis. From C1 to C3 some parameter concentrations increase (TDS, EC, Cl^-, Na^+, Ca^{2+}, Mg^{2+}, K^+, HCO_3^-, F^-, Br^- and SO_4^{2-}), while others decrease (pH and DO). C1 groups the water samples with the lowest salinity values (TDS = 567.2 mg/L); samples belonging to C2 and C3 clusters have higher values (TDS = 933.4 mg/L and 2,938 mg/L, respectively) than C1 samples. HFs classification (Fig. 5) shows that waters of the C1 group mostly belong to Ca-HCO_3 and MixCa-HCO_3 (f3, f4 and FW) HF, those of the C2 group are predominantly MixNa-Cl and MixNa-MixCl (i2 and i3). While waters of the C3 group are nearly all Na-Cl (i3, i4 and SW). This means that C1 groundwaters mark the areas of recharge characterized by freshening processes, whereas those of C2 and C3, qualified by higher concentrations of Cl^-, Na^+, K^+ and SO_4^{2-}, outline the zones subject to saltwater/seawater encroachment. The results of R-mode FA, summarized in Table 3, emphasize that groundwater salinization is the major phenomenon altering the groundwater quality in the SAL aquifer. Table 3 demonstrates that the highest factor loadings associated to F1, which explain 48.26% of total variation, are Na^+ (0.973), Cl^- (0.968), EC (0.930) and Mg^{2+} (0.986). The HFE analysis likewise corroborates that groundwater salinization is acting within the SAL aquifer (Fig. 5).

Results of Q-mode HCA were spatially plotted to illustrate the spatial distribution of groundwater types, as well as to understand their variations over the six sampling surveys from 2016 to 2018 investigating the dynamics of groundwater salinization (Figs. 6 and 7). These thematic maps are prepared by interpolating FSs related to F1 (groundwater salinization) derived by R-mode FA (left-hand side), as well as HFs derived by the HFE analysis (right-hand side). The spatial interpolation of FSs derived by R-mode FA enables distinguishing the areas more affected by F1 (groundwater salinization) as FSs increase, and those less affected by F1 as FSs decrease. The spatial interpolation of sub-phases derived by the HFE-D permits distinguishing areas dominated by freshening processes, as well as those dominated by intrusion sub-phases.

Figs. 6 and 7 show that the areas with negative FS as well as those associated with freshening sub-phases of the HFE classification are generally in the central part of the SAL aquifer. Since most of the C1 samples occur in these zones, the results of the statistical methods and HFE analysis concur in defining the recharge areas of the SAL aquifer, which are associated with the lowest values of TDS, dominated by freshening processes and unaffected by F1. The extension and the position of recharge areas do not significantly change over time. One recharge area is on the NW border of SAL, which is linked to the high altitudes of the contiguous Murgia aquifer (Figs. 1a and 1b). It appears disconnected from the major recharge area of the SAL aquifer, corresponding to the central part of Lecce Province and nearly coinciding with the endorheic part of the territory. One other recharge area, which appears separated from the others, is in the southern part of the SAL aquifer. Disconnections between recharge areas suggest the likely barrier role exerted by the major faults, corroborating the hypothesis of compartmentalization of the SAL aquifer (Fidelibus and Pulido-Bosch, 2019).

The areas with positive values of FS (Figs. 6 and 7) correspond to those marked by C2 and C3 water samples and salinization sub-phases (i1, i2, i3, i4 and SW). These areas are along the Ionian coastline (the left-hand coastline of the SAL aquifer) and within two strips extending from the Ionian to the Adriatic seas in the northern and southern parts of the SAL aquifer. As confirmed by previous studies (Regione Puglia, 2005; 2015; Polemio, 2016), a narrow strip affected by groundwater salinization extends from the Ionian to the Adriatic seas between the Murgia and SAL aquifers.

Fig. 8 summarizes the results of the six sampling surveys. It outlines the spatial distribution of areas with invariant features over time. Moreover, it permits the definition of the areas with a changeover of groundwater characteristics displaying salinization dynamics. Fig. 8 merges information from Fig. 9 outlining areas characterized by the following characteristics:

- areas with FS < 0 (progressive lower effects of groundwater salinization as F1 decreases);
- areas with FS > 1 (progressive higher effects of groundwater salinization as F1 increases);
- areas with freshening HF sub-phases (f1, f2, f3, f4 and FW); and
- areas with salinization HF sub-phases (i3, i4 and SW).

Fig. 8 shows that there is an overlap of areas with FS < 0 and dominated by the presence of freshening HF sub-phases (f1, f2, f3, f4 and FW), as well as areas with FS > 1 and displaying salinization HF sub-

phases (i3, i4 and SW). These zones are characterized by null or minimal HF dynamics and display null or low change over time. Figs. 9a and 9b compare the temporal evolution of FSs and HFs for the wells related to the overlapping zones. Although FSs can be slightly variable over time, the related HFs are stable. The intersection between the zones with FSs < 0 and those dominated by the presence of freshening sub-phases (f1, f2, f3, f4 and FW) enables the delineation of three recharge areas. The intersection between the areas with FS > 1 and displaying salinization sub-phases (i3, i4 and SW) outline the zones subject to groundwater salinization that show stable features during the investigated period (2016-2018).

The intermediate area between the two zones previously defined (yellow areas within the limit of data interpolation of Fig. 8) shows fluctuations in space and time of HFs and FSs (including i1 and i2, which only appear in this area). Some water samples in this area display a high variability of FSs and HFs, which pass from freshening to intrusion sub-phases when FS significantly increases (Fig. 9c). The following decrease of FSs does not always restore previous groundwater quality. Other water samples in Fig. 9d show slightly positive values of FSs, ranging from -0.5 to 1, with low variability over time, but their associated HFs exhibit high variability with a change from freshening to intrusion HFs and vice versa. Based on these findings, the intermediate area shows to be the place of the spatial and temporal dynamics of groundwater salinization.

Thus, Fig. 8 may be the base for a preliminary hazard map related to the groundwater salinization processes occurring in the SAL aquifer. It considers the spatial and temporal variability of salinization phenomena regarding the monitored period (2016-2018), with changes expected because of ongoing climate change and new monitoring data. We highlight that the survey period coincided with the beginning of a long drought period lasting until today without an appreciable recharge (Balacco et al., 2022).

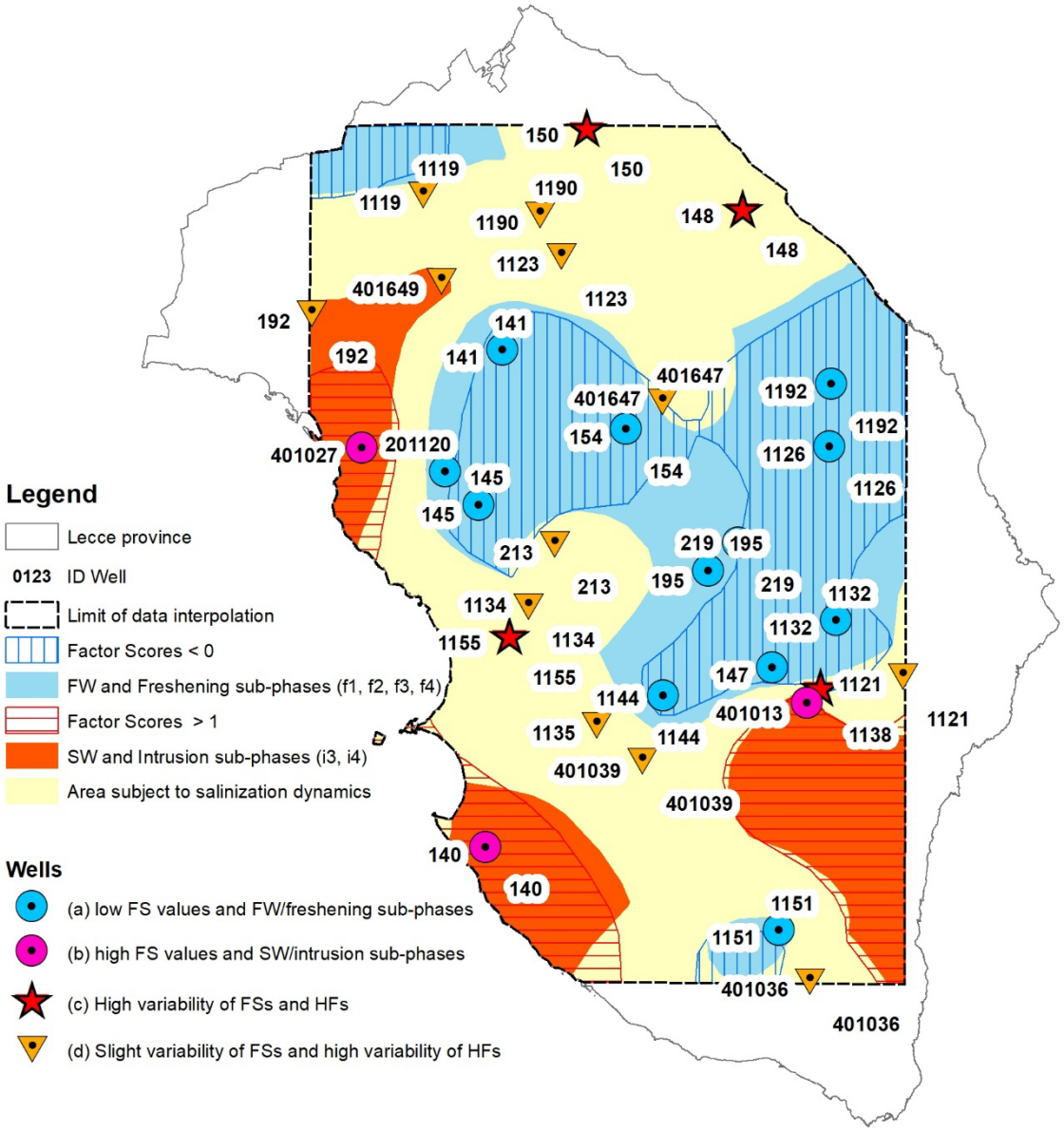

Figure 8. Spatial distribution of areas demonstrating invariant features, as well as areas subject to salinization dynamics over time, and summary of statistical and geochemical characteristics of water samples collected from each well (see Fig. 9).

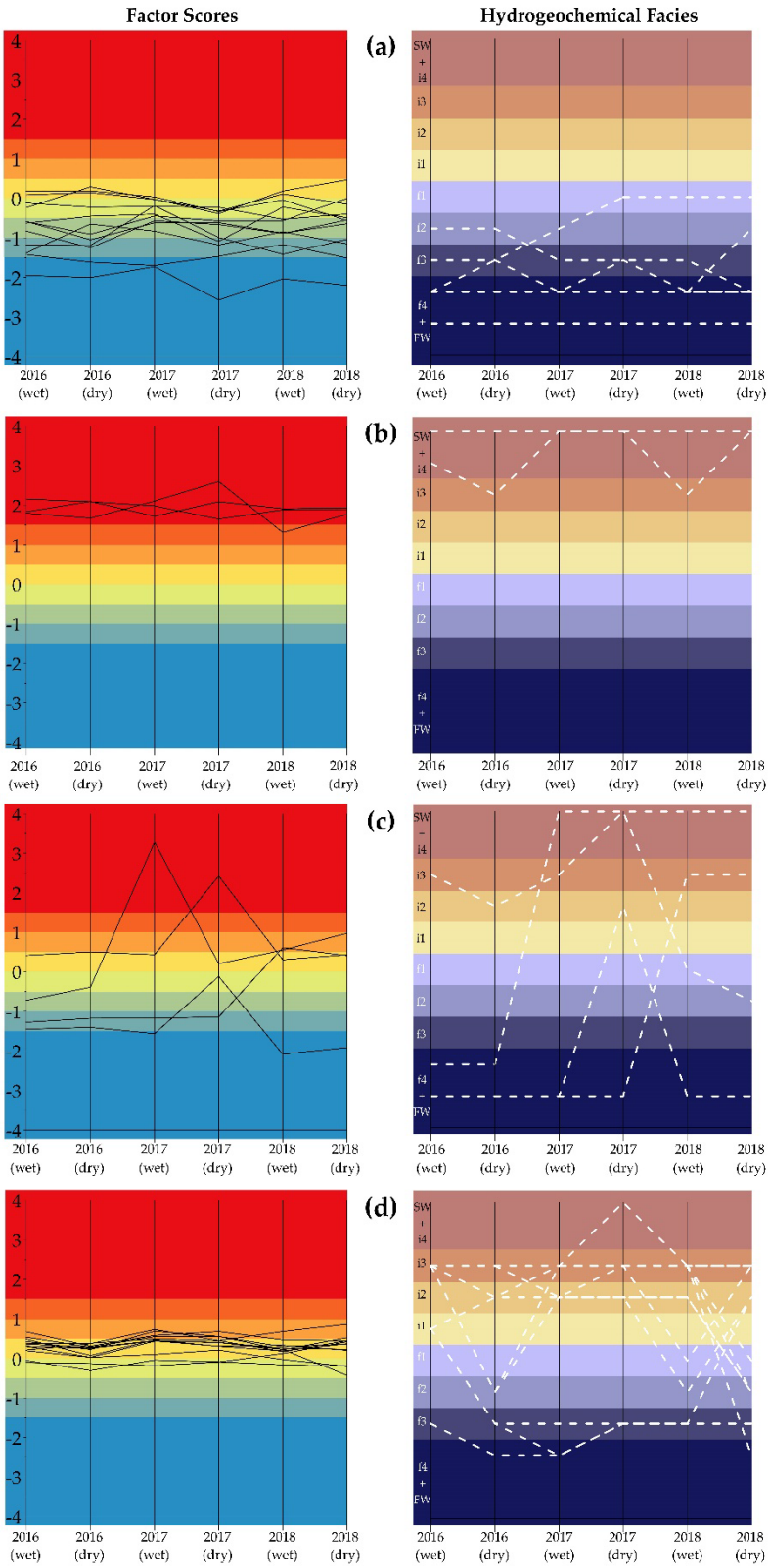

Figure 9. Comparison between FSs (left) and HFs (right) for different water types: (a) low FS values and only FW/freshening sub-phases; (b) high FS values and only SW/intrusion sub-phases; (c) High variability of FSs and HFs; (d) High variability of HFs associated to a slight variation of FSs. Background colours of both sides are the same as Figs. 6 and 7.

Areas with FS < 0 and dominated by FW and freshening facies are of great interest for water management concerning the protection of freshwater resources. Regarding the zones with FS > 1 and dominated by intrusion sub-phases (i3, i4 and SW), even if their condition is driven by the natural low hydraulic heads and water is not used for domestic purposes, could be subject to recovery plans. The intermediate area of Fig. 8 between the two invariant zones and within the limits of data interpolation is characterized by high variability of HFs over time and, consequently, by high salinization dynamics in the investigated period. This last zone should be the focus of further studies to clarify the reasons for such dynamics, as well as for water management policies especially aimed at managing groundwater abstractions.

It is worth illustrating some shortcomings of this study and some general methodological matters deriving from considering them. First, it is apparent that the amount of data and the spatial distribution of the water samples influence the spatial resolution of the results. If the density of the present RMN may be enough for responding to the law, a more homogeneous and denser spatial distribution of sampling points is essential, as suggested by the map of Fig. 8, to refine the understanding of the areas showing variable dynamics of salinization. As a general methodological aspect, the study results show that historical multi-temporal monitoring data comprising basic chemical parameters, also drawn from imperfect well networks, may give valuable information on the generality of salinization phenomena and related dynamics. In subsequent phases, results can guide the implementation of new monitoring points to focus on emerging issues.

Regarding the persisting salinization concerning a few wells in Fig. 9b, this may not be surprising for samples collected from those wells near the coast (wells 140 and 401027), while it should be clarified for well 401013, which is located inland. The latter is a private pumping well with scarce technical information: it could suffer from a short circuit between groundwater preferential levels having different salinity and hydraulic heads, causing vertical flow in the well. To get water quality information with a hydrogeological significance, the sampling at the RMN of the SAL aquifer relies on knowledge of both stratigraphy and well equipment (well casing, screen position) and pump depth (in case of pumping wells). With static wells, the sampling always occurs at the same depth, which roughly corresponds to 5-10 m under the mean water level when groundwater is phreatic (in this case, wells have long screen lengths) or, with locally confined conditions, to the saturated zone thickness captured by a specific screen. With pumping wells, samples come

435 from the pump outlet with known pump installation depth. Although the data derived from sampling at
436 different depths and wells with variable technical features (static or private wells equipped with pumps) may
437 appear to be non-homogeneous, we may reliably use the related information on water quality by checking the
438 elevation of sampling (almost always corresponding to the more productive preferential levels) and knowing
439 the hydro-stratigraphic context. The repetition of the sampling in the same places and at the same depths
440 allows for verifying the qualitative evolution of groundwater over time. This monitoring framework
441 represents the maximum level of homogeneity of information for an aquifer that presents heterogeneity and
442 anisotropy of hydraulic conductivity. Concerning general monitoring rules, the experience says reliable
443 information should depend on knowledge of the equipment of wells. A good deal of the worldwide available
444 monitoring data does not go with this type of information, notwithstanding the diffuse heterogeneity and
445 anisotropy of most aquifers.
446 In general, the coastal nature of groundwater makes sampling reliability even more challenging. For
447 example, Fig. 10 shows the log of the specific conductivity profile for a fully screened well with no vertical
448 flow (no. 154, in the middle of the SAL aquifer and drilled where groundwater is phreatic). It reaches
449 saltwater at its bottom beneath freshwater and transition zones. The specific conductivity profile provides
450 evidence for the issues in groundwater sampling in coastal aquifers, which may be devised by the three-
451 dimensional distribution of salinity. Fig. 10 also shows the Schoeller diagram of water samples collected in
452 1986 during a multi-vertical sample survey from the former Hydrogeology Laboratory of the University of
453 Bari - (data available in the MEDSAL Observatory at https://medsal.eu/observatory/). Parameter
454 concentrations and specific conductivity vary according to sampling depth: samples collected from -88 m
455 AMSL to -155 m AMSL, representing brackish waters of the transition zone and salt waters, demonstrate an
456 increasing salt content.
457 Thus, the representativeness of groundwater samples drawn from a coastal aquifer may depend not only
458 on the equipment of each well but also on the sampling depth (or location of pumps). If in a coastal aquifer
459 that shows heterogeneity and anisotropy of the hydraulic conductivity the three-dimensional location of the
460 sample within groundwater is unclear, randomness may lead to comparing groundwater samples that are not
461 correlated from the hydrogeological point of view. A groundwater sample dataset with such characteristics
462 conditions the results of statistical and HFE methods, as well as of any other interpretation method.

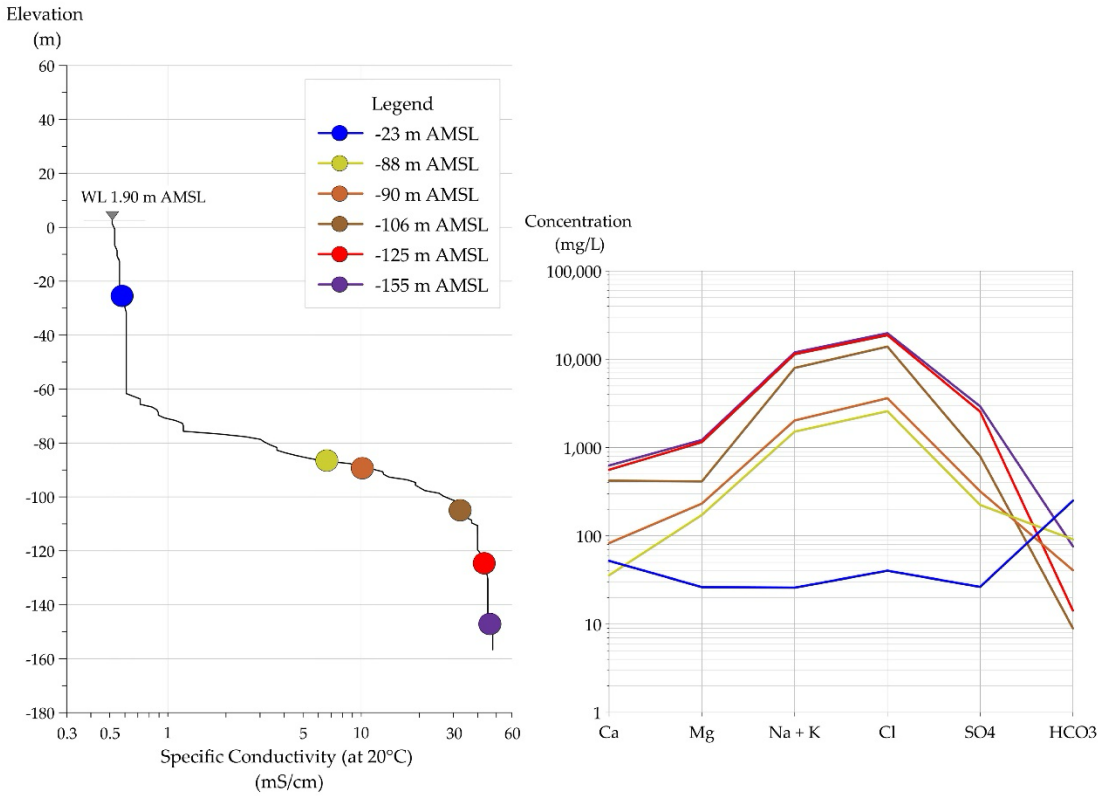

Figure 10. Specific conductivity profile and Schoeller diagrams for six water samples collected at different depths from the fully screened well 154 (in the central part of SAL aquifer) that reaches saltwater beneath freshwater and transition zone.

Being aware of these aspects, as well as the heterogeneity and anisotropy of the SAL aquifer concerning its geological setting, sampling protocols used for the six sampling surveys considered in this study ensure such significance for almost all samples. Overall, the proposed approach remains useful as a preliminary evaluation of groundwater hazard assessment related to the salinization phenomenon and its variation in time and space.

6. Conclusions

This study aimed to investigate the groundwater salinization dynamics concerning a karstic coastal aquifer (SAL aquifer, Southern Italy) located in the Mediterranean basin. To this end, we applied statistical (Q-mode HCA and R-mode FA) and hydrogeochemical methods (HFE analysis) and compared the results with a novel concept. The data analysis led to a preliminary hazard map related to groundwater salinization, which considers the spatial and temporal variability of the salinization processes.

Concerning the monitoring period (2016-2018), the overview of both statistical and hydrogeochemical results enabled the outline of areas with null or minimal freshening/salinization dynamics, and of areas highly affected by the changeover of HFs from freshening to intrusion sub-phases and vice versa. The former show invariant features: the freshening or intrusion processes are steady. Concerning the latter, the dynamics of groundwater salinization are straightforward. The comparison of results demonstrated that, even if based on different methodological approaches, the statistical and geochemical methods validate each other, showing both comparable and complementary results in defining recharge areas and those subject to saltwater intrusion and salinization.

Considering the discussed sampling issues and given that parameter concentrations significantly influence both the statistical and hydrogeochemical analyses, these methods, as a general guideline, should be applied with caution to coastal aquifers. A thorough geological and technical knowledge of the groundwater monitoring network concerning the equipment of wells, drilling stratigraphy, position of screens, elevation of pumps, and sampling depths is needed for solving these issues. When monitoring networks and sampling protocols are reliable, the proposed approach may be very efficient for the preliminary evaluation of the hazard assessment of the spatial and temporal dynamics of groundwater salinization.

Acknowledgements

This research is conducted in the context of MEDSAL Project© (www.medsal.eu), which is part of the PRIMA Programme supported by the European Union's Horizon 2020 Research and Innovation Programme and funded by the national funding agencies of MIUR (Grant number: 1421) and TÜBİTAK (Grant number: 118Y366).

References

Alfio, M.R., Balacco, G., Parisi, A., Totaro, V., Fidelibus, M.D., 2020. Drought index as indicator of salinization of the Salento Aquifer (Southern Italy). Water 12(1927). https://doi.org/10.3390/w12071927.

Alther, G.A., 1979. A simplified statistical sequence applied to routine water quality analysis: A case history. Groundwater 17(6), pp. 556–561. https://doi.org/10.1111/j.1745-6584.1979.tb03356.x.

Bahir, M., Ouhamdouch, S., Carreira, P. M., Zouari, K., 2018. Relationship between hydrochemical variation and the seawater intrusion within coastal alluvial aquifer of Essaouira basin (Morocco) using HFE-diagram. In: Chaminé, H., Barbieri, M., Kisi, O., Chen, M., Merkel, B. (eds) Advances in Sustainable and Environmental Hydrology, Hydrogeology, Hydrochemistry and Water Resources. CAJG 2018. Advances in Science, Technology & Innovation. Springer, Cham. https://doi.org/10.1007/978-3-030-01572-5_47.

Bahrami, M., Khaksar, E., Khaksar, E., 2020. Spatial variation assessment of groundwater quality using multivariate statistical analysis (Case study: Fasa Plain, Iran). J. Groundw. Sci. Eng. 8(3), pp. 230–243. https://doi.org/10.19637/j.cnki.2305-7068.2020.03.004.

Balacco, G., Alfio, M.R., Parisi, A., Panagopoulos, A., Fidelibus, M.D., 2022. Application of short time series analysis for the hydrodynamic characterization of a coastal karst aquifer: the Salento aquifer (Southern Italy). J. Hydroinformatics 24(2), pp. 420–443. https://doi.org/10.2166/hydro.2022.135.

Basilevsky, A., 1994. Statistical Factor Analysis and Related Methods. Theory and applications. John Wiley & Sons, New York.

Bear, J., Cheng, A.H.D., Sorek, S., Ouazar, D., Herrera, I., 1999. Seawater Intrusion in Coastal Aquifers-Concepts, Methods, and Practices. In: Bear J, Cheng AHD, Sorek S, Ouazar D, Herrera I (eds) Theory and Applications of Transport in Porous Media. Kluwer Academic Publishers, Dordrecht/ Boston/London, 14, pp. 51–71.

Bouderbala, A., 2015. Groundwater salinization in semi-arid zones: an example from Nador plain (Tipaza, Algeria). Environ. Earth Sci. 73, pp. 5479–5496. https://doi.org/10.1007/s12665-014-3801-9.

Box, G.E., Cox, D.R., 1964. An Analysis of Transformations. J. R. Stat. Soc. Ser. B 26, pp. 211–252. https://doi.org/10.1111/j.2517-6161.1964.tb00553.x.

Box, G.E., Cox, D.R., 1982. An analysis of transformations revisited, rebutted. J. Am. Stat. Assoc. 77(377), pp. 209–210. https://doi.org/10.1080/01621459.1982.10477788.

COST, 2003. COST Action 620 Vulnerability and Risk Mapping for the Protection of Carbonate (Karst) Aquifers; Final Report; Zwahlen, F. (Ed.) European Commission, Directorate-General for Research: Luxembourg, 2004.

Custodio, E., 2010. Coastal aquifers of Europe: an overview. Hydrogeol. J. 18(1), pp. 269–280. https://doi.org/10.1007/s10040-009-0496-1.

Custodio, E., Bruggeman, G.A., 1987. Groundwater problems in coastal areas, UNESCO. International Hydrological Programme.

Dalton, M.G., Upchurch, S.B., 1978. Interpretation of hydrochemical facies by factor analysis. Groundwater 16, pp. 228–233. https://doi.org/10.1111/j.1745-6584.1978.tb03229.x.

Davis, J.C., 1986. Statistics and Data Analysis in Geology, 2nd ed., Wiley, New York.

Domínguez, P., Custodio, E., 1992. Sea water intrusion in the lower north–eastern aquifer of the "Campo de Dalías" (Almería, South-eastern Spain): preliminary study of monitoring data. 12th SWIM, Barcelona, pp. 631–659.

Farnham, I.M., Singh, A.K., Stetzenbach, K.J., Johannesson, K.H., 2002. Treatment of nondetects in multivariate analysis of groundwater geochemistry data. Chemom. Intell. Lab. Syst. 60, pp. 265–281. https://doi.org/10.1016/S0169-7439(01)00201-5.

Fidelibus, M.D., Calò, G., Tinelli, R., Tulipano, L., 2011. Salt ground waters in the Salento karstic coastal aquifer (Apulia, Southern Italy). In: Lambrakis, N., Stournaras, G., Katsanou, K. (eds) Advances in the Research of Aquatic Environment. Environ. Earth Sci., pp. 407–415, Springer, Berlin, Heidelberg. https://doi.org/10.1007/978-3-642-19902-8_48.

Fidelibus, M.D., Tulipano, L. (1986). Mixing phenomena owing to sea water intrusion for the interpretation of chemical and isotopic data of discharge waters in the Apulian coastal carbonate aquifer (southern Italy). Salt water intrusion meeting. 9. pp. 591-600.

Fidelibus, M.D., Pulido-Bosch, A., 2019. Groundwater temperature as an indicator of the vulnerability of Karst coastal aquifers. Geosciences 9, 23. https://doi.org/10.3390/geosciences9010023.

Ghesquière, O., Walter, J., Chesnaux, R., Rouleau, A., 2015. Scenarios of groundwater chemical evolution in a region of the Canadian Shield based on multivariate statistical analysis. J. Hydrol. Reg. Stud. 4, pp. 246–266. https://doi.org/10.1016/j.ejrh.2015.06.004.

Giménez-Forcada, E., 2010. Dynamic of seawater interface using hydrochemical facies evolution diagram. Groundwater 48(2), pp. 212–216. https://doi.org/10.1111/j.1745-6584.2009.00649.x.

Giménez-Forcada, E., 2014. Space/time development of seawater intrusion: A study case in Vinaroz coastal plain (Eastern Spain) using HFE-Diagram, and spatial distribution of hydrochemical facies. J. Hydrol. 517, pp. 617–627. https://doi.org/10.1016/j.jhydrol.2014.05.056.

Giménez-Forcada, E., Sánchez San Román, F. J., 2015. An Excel Macro to Plot the HFE-Diagram to Identify Sea Water Intrusion Phases. Groundwater, 53(5), pp. 819-824. https://doi.org/10.1111/gwat.12280.

Giménez-Forcada, E., 2019. Use of the Hydrochemical Facies Diagram (HFE-D) for the evaluation of salinization by seawater intrusion in the coastal Oropesa Plain: Comparative analysis with the coastal Vinaroz Plain, Spain. HydroResearch 2, pp. 76–84. https://doi.org/10.1016/j.hydres.2019.11.007.

Gleick, P.H., Ajami, N., Christian-Smith, J., Cooley, H., Donnelly, K., Fulton, J., Ha, M.L., Heberger, M., Moore, E., Morrison, J., Orr, S., Schulte, P., Srinivasan, V., 2014. The World's Water, The biennial report on freshwater resources (Vol. 8). Island press.

Güler, C., Thyne, G.D., McCray, J.E., Turner, A.K., 2002. Evaluation of graphical and multivariate statistical methods for classification of water chemistry data. Hydrogeol. J. 10, pp. 455–474. https://doi.org/10.1007/s10040-002-0196-6.

Hajji, S., Allouche, N., Bouri, S., Aljuaid, A. M., & Hachicha, W., 2021. Assessment of Seawater Intrusion in Coastal Aquifers Using Multivariate Statistical Analyses and Hydrochemical Facies Evolution-Based Model. International Journal of Environmental Research and Public Health, 19(1), 155. https://doi.org/10.3390/ijerph19010155.

581 Johannesson, K.H., Stetzenbach, K.J., Kreamer, D.K., Hodge, V.F., 1996. Multivariate statistical analysis of
582 arsenic and selenium concentrations in groundwaters from south-central Nevada and Death Valley,
583 California. J. Hydrol.178(1–4), pp. 181–204. https://doi.org/10.1016/0022-1694(95)02804-8.

584 Johnson, R.A., Wichern, D.W., 1992. Applied Multivariate Statistical Analysis. 3rd ed., Prentice-Hall
585 International, Englewood Cliffs, New Jersey.

586 Kaiser, H.F., 1974. An index of factorial simplicity. Psychometrika 39, pp. 31–36.
587 https://doi.org/10.1007/BF02291575.

588 Kaiser, H.F., 1981. A revised measure of sampling adequacy for factor-analytic data matrices. Educ.
589 Psychol. Meas. 41(2), pp. 379–381. https://doi.org/10.1177/001316448104100216.

590 Kim, J.H., Kim, R.H., Lee, J., Cheong, T.J., Yum, B.W., Chang, H.W., 2005. Multivariate statistical analysis
591 to identify the major factors governing groundwater quality in the coastal area of Kimje, South Korea.
592 Hydrol. Process. 19(6), pp. 1261–1276. https://doi.org/10.1002/hyp.5565.

593 Kolmogorov, A.N., 1933. Sulla Determinazione Empirica di Una Legge di Distribuzione, Giornale
594 dell'Istituto Italiano degli Attuari 4, pp. 83–91.

595 Leduc, C., Pulido-Bosch, A., Remini, B., Massuel, S., 2016. Changes in Mediterranean groundwater
596 resources. In The Mediterranean Region under Climate Change; IRD, Ed.; IRD Editions: Marseille, pp.
597 328–333. ISBN 978-2-7099-2219-7.

598 Machiwal, D., Cloutier, V., Güler, C., Kazakis, N., 2018. A review of GIS-integrated statistical techniques
599 for groundwater quality evaluation and protection. Environ. Earth Sci. 77(19), Article Number: 681.
600 doi:10.1007/s12665-018-7872-x.

601 Mastrocicco, M., Colombani, N., 2021. The Issue of Groundwater Salinization in Coastal Areas of the
602 Mediterranean Region: A Review. Water 13, 90. https://doi.org/10.3390/w13010090.

603 Muzzillo, R., Zuffianò, L.E., Rizzo, E., Canora, F., Capozzoli, L., Giampaolo, V., De Giorgio, G., Sdao, F.,
604 Polemio, M., 2021. Seawater intrusion proneness and geophysical investigations in the Metaponto
605 coastal plain (Basilicata, Italy). Water 13, 5. https://doi.org/10.3390/w13010053.

606 Pacheco Castro, R., Pacheco Ávila, J., Ye, M., Cabrera Sansores, A., 2018. Groundwater quality: analysis of
607 its temporal and spatial variability in a karst aquifer. Groundwater 56(1), pp. 62–72.
608 https://doi.org/10.1111/gwat.12546.

609 Papatheodorou, P.G., Lambrakis, N., Panagopoulos, G., 2007. Application of multivariate statistical
610 procedures to the hydrochemical study of a coastal aquifer: an example from Crete, Greece. Hydrol.
611 Process. 21(11), pp. 1482–1495. https://doi.org/10.1002/hyp.6322.

612 Parisi, A., Monno, V., Fidelibus, M.D., 2018. Cascading vulnerability scenarios in the management of
613 groundwater depletion and salinization in semi-arid areas. Int. J. Disaster Risk Reduct. 30, pp. 292–
614 305. https://doi.org/10.1016/j.ijdrr.2018.03.004.

615 Pescaroli, G., Alexander, D., 2015. A definition of cascading disasters and cascading effects: Going beyond
616 the "toppling dominos" metaphor. Planet@ risk 3(1), pp. 58–67.

617 Pescaroli, G., Nones, M., Galbusera, L., Alexander, D., 2018. Understanding and mitigating cascading crises
618 in the global interconnected system. Int. J. Disaster Risk Reduct. 30, pp. 159–163.

Petalas, C., Lambrakis, N., 2006. Simulation of intense salinization phenomena in coastal aquifers-the case of the coastal aquifers of Thrace. J. Hydrol. 324(1–4), pp. 51–64. https://doi.org/10.1016/j.jhydrol.2005.09.031.

Regione Puglia, 2005. Piano di Tutela delle acque – I Ciclo (Water protection plan – I Cycle). Available at: http://www.sit.puglia.it/portal/portale_pianificazione_regionale/Piano%20di%20Tutella%20delle%20Acque [accessed 19 October 2022]

Regione Puglia, 2015 – Piano di Tutela delle acque – II Ciclo (Water protection plan – II Cycle). Available at: http://www.sit.puglia.it/portal/portale_pianificazione_regionale/Piano%20di%20Tutella%20delle%20Acque [accessed 19 October 2022]

Piper, A.M., 1944. A graphic procedure in the geochemical interpretation of water-analyses. Transactions, American Geophysical Union 25, 914-923.

Polemio, M., 2016. Monitoring and management of karstic coastal groundwater in a changing environment (Southern Italy): A review of a regional experience. Water 8, 148. https://doi.org/10.3390/w8040148.

Prusty, P., Farooq, S.H., 2020. Seawater intrusion in the coastal aquifers of India-A review. HydroResearch 3, pp. 61–74. https://doi.org/10.1016/j.hydres.2020.06.001.

Pulido-Bosch, A., Navarrete, F., Molina, L., Martinez-Vidal, J.L., 1991. Quantity and quality of groundwater in the Campo de Dalias (Almeria, SE Spain). Water Sci. Technol. 24(11), pp. 87–96. https://doi.org/10.2166/wst.1991.0340.

R Core Team, 2019. R: A Language and Environment for Statistical Computing. R Foundation for Statistical Computing, Vienna, Austria. https://www.R-project.org/ [accessed 19 October 2022]

Rahman, A., Mondal, N.C., Tiwari, K.K., 2021. Anthropogenic nitrate in groundwater and its health risks in the view of background concentration in a semi-arid area of Rajasthan, India. Sci. Rep. 11, 9279. https://doi.org/10.1038/s41598-021-88600-1

Reimann, C., Filzmoser, P., 2000. Normal and lognormal data distribution in geochemistry: Death of a myth. Consequences for the statistical treatment of geochemical and environmental data. Environ. Geol. 39, pp. 1001–1014. https://doi.org/10.1007/s002549900081

Roy, S. K., Zahid, A., 2021. Assessment of river water–groundwater–seawater interactions in the coastal delta of Bangladesh based on hydrochemistry and salinity distribution. SN Appl. Sci. 3, 411. https://doi.org/10.1007/s42452-021-04389-8

Romesburg, H.C., 1984. Cluster Analysis for Researchers. Lifetime Learning Publications. Belmont, California.

Sae-Ju, J., Chotpantarat, S., Thitimakorn, T., 2020. Hydrochemical, geophysical and multivariate statistical investigation of the seawater intrusion in the coastal aquifer at Phetchaburi Province, Thailand. Journal of Asian Earth Sciences, 191, 104165. https://doi.org/10.1016/j.jseaes.2019.104165

Sanford, R.F., Pierson, C.T., Crovelli, R.A., 1993. An objective replacement method for censored geochemical data. Math. Geol. 25, pp. 59–80. https://doi.org/10.1007/BF00890676

Sappa, G., De Filippi, F.M., Ferranti, F., Iacurto, S., 2019. Environmental issues and anthropic pressures in coastal aquifers: a case study in Southern Latium Region. Acque Sotterranee-Italian Journal of Groundwater, 8(1). https://doi.org/10.7343/as-2019-373

Schoeller, H., 1955. Géochemie des eaux souterraines. Revue de L'Institute Francais du Pétrole 10, pp. 230–244.

Smirnov, N., 1948. Table for estimating the goodness of fit of empirical distributions. Ann. Math. Stat. 19(2), pp. 279–281. https://doi.org/10.1214/aoms/1177730256

Stiff, H.A., Jr., 1951. The interpretation of chemical water analysis by means of patterns. J. Pet. Technol. 3(10), pp. 15–17.

Struckmeier, W. F., Margat J., 1995. Hydrogeological maps: a guide and a standard legend. International contributions to hydrogeology, 17, International Association of Hydrogeologist, Hannover, Heise. ISBN 3-922705-98-7.

Tadolini, T., Tulipano, L., Fidelibus, M.D., 1982. Significativi aspetti del chimismo delle acque sotterranee circolanti nell'acquifero carsico della penisola Salentina (Italia Meridionale). Geologia Applicata e Idrogeologia, 17, 411-426.

Tamez-Meléndez, C., Hernández-Antonio, A., Gaona-Zanella, P.C., Ornelas-Soto, N., Mahlknecht, J., 2016. Isotope signatures and hydrochemistry as tools in assessing groundwater occurrence and dynamics in a coastal arid aquifer. Environ. Earth Sci. 75, 830. https://doi.org/10.1007/s12665-016-5617-2

Telahigue, F., Agoubi, B., Souid, F., Kharroubi, A., 2018. Assessment of seawater intrusion in an arid coastal aquifer, south-eastern Tunisia, using multivariate statistical analysis and chloride mass balance. Phys. Chem. Earth. 106, 37–46. https://doi.org/10.1016/j.pce.2018.05.001

Tulipano, L., Fidelibus, M.D. 2002. Mechanism of groundwater salinisation in a coastal karstic aquifer subject to over–exploitation. Proc. 17th SWIM, Delft, The Netherlands.

Tulipano, L., Fidelibus, M.D., Panagopoulos, A., 2005. Groundwater management of coastal karstic aquifers, Final Report COST ACTION 621, vol. EUR 21366, p. 1-363, OFFICE FOR OFFICIAL PUBL. OF THE EUROPEAN COMM., ISBN: 92-898-0015-1.Ward, J.H., 1963. Hierarchical Grouping to Optimize an Objective Function. J. Amer. Statist. Assoc. 58(301), pp. 236–244. https://doi.org/10.1080/01621459.1963.10500845.

Werner, A.D., Bakker, M., Post, V.E.A., Vandenbohede, A., Lu, C., Ataie-Ashtiani, B., Simmons, C.T., Barry, D.A., 2013. Seawater intrusion processes, investigation, and management: Recent advances and future challenges. Advances in Water Resources, 51, 3-26, https://doi.org/10.1016/j.advwatres.2012.03.004.